JOURNAL OF Applied Polymer SCIENCE

Reactive Blend of Epoxy-Novolac Resin and Epoxide-Terminated Low-Molecular-Weight Poly(phenylene oxide)

Jingzhao Mo, Lei Xia, Pengju Pan, Baoqing Shentu, Zhixue Weng
State Key Laboratory of Chemical Engineering, Department of Chemical and Biological Engineering, Zhejiang University, Hangzhou 310027, China
Correspondence to: P. Pan (E-mail: panpengju@zju.edu.cn) or B. Shentu (E-mail: shentu@zju.edu.cn)

ABSTRACT: The epoxide-terminated low-molecular-weight poly(phenylene oxide) (PPO), EPPO, was synthesized by modifying the terminal hydroxyl group of PPO and it was reactively blended with epoxy-novolac resin (EPN). The curing kinetics, phase morphology, thermal stability, dielectric property, and water absorption behavior of the cured EPN/EPPO blends were investigated and compared with the unmodified EPN/PPO blends. As revealed by the FTIR and DSC analysis, EPPO takes part in the curing reaction and forms a reactive blend with EPN. The curing rate of both EPN/PPO and EPN/EPPO blends first increases and then decreases with increasing the PPO or EPPO fraction. The blends have lower degree of curing than neat EPN, due to the steric hindrance effects of PPO or EPPO. Because of the reaction between blend components, EPN/EPPO blends show faster curing rate and higher degree of curing than the corresponding EPN/PPO blends. The reactive blending improves the dispersion of EPPO in EPN matrix and the EPN/EPPO blend forms a co-continuous morphology even at a low EPPO content, compared to the typical sea-island morphology of the EPN/PPO blend. The EPN/EPPO blend has remarkable smaller dielectric constant, dissipation factor, and water absorption than neat EPN. © 2012 Wiley Periodicals, Inc. J. Appl. Polym. Sci. 000: 000–000, 2012

KEYWORDS: poly(phenylene oxide); epoxy-novolac resin; curing kinetics; phase morphology

Received 15 April 2012; accepted 22 May 2012; published online
DOI: 10.1002/app.38101

INTRODUCTION

Epoxy resins are an important class of thermosetting materials with good mechanical and electrical properties, excellent heat, water, and chemical resistances, and have been widely used as the materials of electronic devices.[1,2] However, the applications of epoxy resins in the high-performance electronic products that request fast transportation speed and high circuit density are restrained because of their inferior thermal and dielectric properties.[3,4] Polymer blending has been a feasible and convenient way to improve the physical properties of epoxy resins. Epoxy resins have been blended with several polymers such as poly(phenylene oxide) (PPO),[5–16] cyanate ester (CE),[17–19] and polyimide.[20,21] Among them, PPO has the good heat-resistant property, high dimensional stability, low moisture uptake, low flammability, as well as the excellent electrical properties such as low dielectric constant and dissipation factor.[5,6] Therefore, the epoxy/PPO blend has been considered as an excellent candidate for the high-performance electrical materials, e.g., high-frequency substrates.

The miscibility and phase behavior of epoxy/PPO blend system have been investigated by several research groups.[6–10] PPO is thermodynamically immiscible with epoxy resin, and therefore the phase separation occurs in their blends, which is more significant for the PPO with high molecular weight. Prolongo et al.[9] and Soulé et al.[10] have found that the molecular weight of PPO influences its miscibility with epoxy resin and the decrease of PPO molecular weight leads to the improvement of miscibility, due to the larger entropic contribution to the free energy of mixing. Ishii et al.[11] have studied the correlations between the phase separation and curing reaction of epoxy/PPO blends and found that the curing reaction promotes the phase separation, because of the formation of cross-linked structure and the increase of molecular weight of epoxy resin during curing.

Reactive blending of immiscible polymers is a useful strategy to produce the polymeric materials with the controlled phase morphology and high physical performances.[22–24] The compatibilizers such as styrene-maleic anhydride random copolymer[6] and triallylisocyanurate[12,13] have been introduced into the epoxy/PPO blends to construct the reactive blends. These compatibilizers connect the immiscible polymer molecules through forming enhanced entanglements on both sides of the interface.

Applied Polymer SCIENCE

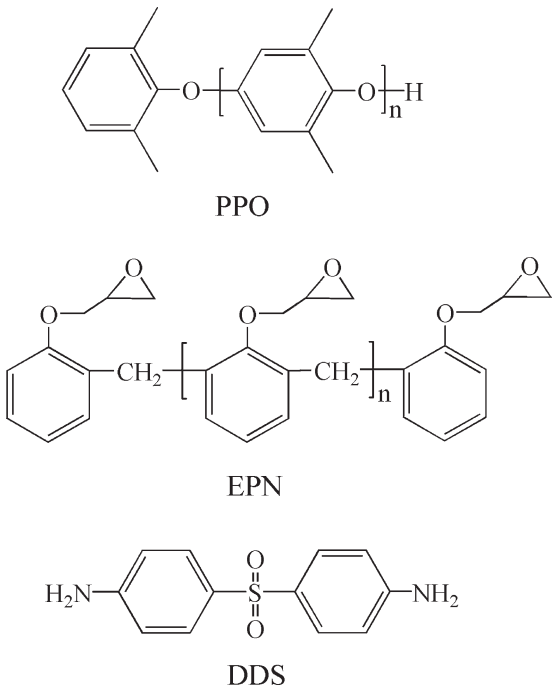

Scheme 1. Chemical structures of PPO, EPN, and DDS.

Besides, the chemical functionalization of polymer chains is a widely used method to achieve the reactive blend. The reactive functional groups can react to form block or graft copolymers at the interface, which can reduce the interfacial tension and stabilize the morphology of blends. In the case of PPO, the functional groups such as epoxide,[5] fumaric acid,[7] and (di-*n*-butylamino) methyl[14] have been attached to its chain ends or polymer backbones. Merfeld et al.[7] have reported that the acid-graft of PPO plays a dominant role in determining the size of dispersed phase and reduces the miscibility of epoxy/PPO blends because of the more endothermic interaction energy. At present, the effects of terminal modification of PPO and reactive blending on the phase morphology of epoxy/PPO blends are far from being well understood.

Curing kinetics and conditions are usually the key factors influencing the degree of curing and phase behavior, as well as the physical properties of thermoset plastics and their blends. However, the curing kinetics of epoxy/PPO blends as well as their dependence on the reaction between the blend components has been scarcely investigated. The phenol-formaldehyde epoxy-novolac resin (EPN) has greatly improved chemical and heat resistance compared with the much more common bisphenol-A epoxy resin[25,26] and would be more suitable for the applications as high-performance electrical materials. Despite the extensive studies on the blends of bisphenol-A epoxy resin and PPO, the EPN/PPO blend system has not been explored.

In this study, the epoxide-terminated low-molecular-weight PPO was synthesized and blended with EPN. The nonisothermal and isothermal curing kinetics, phase morphology, thermal decomposition, dielectric property, and water absorption behavior of EPN/EPPO blends were investigated and compared with the unmodified EPN/PPO blends. The effects of reactive blending and terminal modification of PPO on the curing behavior and phase morphology of EPN/PPO blends were discussed.

EXPERIMENTAL

Materials

Poly(2,6-dimethyl-1,4-phenylene oxide) (PPO, SA120) with a viscosity of 7340 Pas was purchased from the Saudi Basic Industry Corp. EPN (D.E.N. 431) with a multiepoxy functionality of 2.8 and an epoxy equivalent weight of 172–179 g/eq was purchased from Dow Chemical Company. The curing agent 4,4′-diaminodiphenylsulfone (DDS), epichlorohydrin, and 2-methoxyethanol were purchased from Aladdin Reagent Co. All reagents were used as received. The chemical structures of EPN, PPO, and DDS are illustrated in Scheme 1.

Synthesis of Epoxide-Terminated PPO

Scheme 2 illustrates the synthetic procedure of epoxide-terminated PPO (EPPO). The terminal epoxidation of PPO was carried out in a 150-mL three-necked round-bottomed flask equipped with a reflux condenser and thermometer. In run 1, 3.0 g PPO was dissolved in a mixture of 5 mL 2-methoxyethanol and 30 mL epichlorohydrin. The reaction mixture was heated to 70°C under vigorous stirring and 3 mL of 30% aqueous NaOH solution dissolved in 5 mL 2-methoxyethanol was added dropwise over a period of 1 h. The reaction mixture was then stirred at 70°C for 3 h. After the reaction, the mixture was poured into a mixed solvent containing 300 mL methanol and 150 mL deionized water. The filtrated product was dried at 50°C for 24 h under vacuum. In run 2, the reaction temperature of 90°C was used instead. The epoxide-terminated PPO is marked as EPPO(x), where x represents the conversion of terminal group of PPO determined from the NMR analysis.

Preparation of EPN and Its Blends

PPO (or EPPO), EPN, and DDS with the predetermined weights (Table I) were dissolved in a mixed solvent of 5 mL chloroform and 5 mL acetone. The solvent was removed under ventilating cabinet at room temperature for 48 h and under vacuum at 40°C for 24 h. The blends freshly prepared were directly used for the differential scanning calorimetry (DSC)

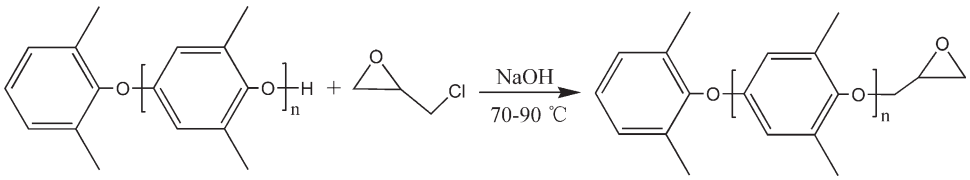

Scheme 2. Synthetic route of EPPO.

Table I. Composition of the Blends

Sample	PPO (g)	EPPO (g)	EPN (g)	DDS (g)
EPN	0	0	1.00	0.36
EPN/PPO-0.1	0.10	0	0.90	0.32
EPN/PPO-0.3	0.30	0	0.70	0.25
EPN/PPO-0.5	0.50	0	0.50	0.18
EPN/EPPO-0.1	0	0.10	0.90	0.33
EPN/EPPO-0.3	0	0.30	0.70	0.26
EPN/EPPO-0.5	0	0.50	0.50	0.19

analysis. For the analyses of phase morphology and physical properties, the blends freshly prepared were poured into a mold and cured in a vacuum oven with successive annealing at 80°C for 1 h, 120°C for 2 h, 160°C for 1 h, and 200°C for 2 h. In the EPN/EPPO blends, only the EPPO with a high degree of epoxidation, i.e., EPPO (1.0), was used. The blends are marked as EPN/PPO-*y* or EPN/EPPO-*y*, where *y* corresponds to the weight fraction of PPO or EPPO.

Characterization

^{1}H-NMR spectra were recorded on a 300 MHz Bruker AVANCE II nuclear magnetic resonance spectrometer (Bruker BioSpin Corporation, Switzerland) using $CDCl_3$ as the solvent.

The number- and weight-averaged molecular weight (M_n, M_w) and polydispersity index (PDI) were determined by a Waters 1525/2414 gel permeation chromatography (GPC, Waters Instruments, USA) equipped with a Waters Styragel HT4/HT3/HR1 columns and a refractive index detector. The mobile phase was toluene with a flow rate of 1.0 mL/min. The column temperature was set at 30°C. The molecular weight was calibrated by the polystyrene standards.

The calorimetric measurements were performed on a PE DSC-7 instrument (Perkin-Elmer Corp., USA). The sample with a weight of 5–10 mg was encapsulated into an aluminum pan. In the nonisothermal curing process, the sample was heated from 30 to 300°C at a heating rate of 5°C/min. The peak top in the nonisothermal DSC curves was taken as the curing temperature. In the isothermal curing procedure, the sample was heated from 30 to 180°C at a heating rate of 100°C/min and then held at this temperature for 40 min for curing. The peak areas in the nonisothermal and isothermal DSC curing curves were taken as the curing enthalpy (ΔH_c). The ΔH_c values were normalized by the weight of EPN component.

Fourier transform infrared (FTIR) spectroscopic analysis was carried out on a NICOLET 5700 spectrometer (Thermo Electron Corp., USA). The spectrum was collected in the frequency range of 400–4000 cm^{-1} with a resolution of 4 cm^{-1} by averaging 16 scans.

The phase morphology of blends was examined with a Hitachi TM-1000 scanning electron microscope (Hitachi Corp., Japan). To clearly see the phase behavior, the cryofracture surface of blends was etched in chloroform for 4 h at 25°C to remove the PPO or EPPO component.

Thermogravimetric analysis (TGA) was performed on a PE Pyris 1 TGA (Perkin-Elmer Corp., USA) under a nitrogen atmosphere. The sample with a weight of ~ 10 mg was placed in a platinum pan and was heated from 30 to 700°C at a rate of 10°C/min.

The dielectric characterization was conducted by the parallel-plate capacitor method with a Turnkey Concept 80 dielectric spectrometer (Novocontrol Tech. GmbH & Co. KG, Germany) on the silver-pasted sample. The measurements were performed at 25°C in a frequency of 1 MHz.

To analyze the water absorption behavior, the sample was first dried at 120°C for 6 h under vacuum. After cooling down to 25°C, the sample was weighed, then immersed into the boiling water for 48 h, and finally weighed. The water uptake was calculated as follows

$$\text{Wateruptake } (\%) = (W/W_0 - 1) \times 100\%$$

where W and W_0 are the weights of sample after and before water absorption, respectively.

RESULTS AND DISCUSSION

Synthesis of EPPO

EPPO was prepared by an epoxidation reaction between the terminal hydroxyl group of PPO and epichlorohydrin using NaOH as a catalyst.[5,27] The structures of original and terminally modified PPO were confirmed by ^{1}H-NMR, as shown in Figure 1. The NMR result of PPO and EPPO is shown as follows.

PPO, ^{1}H-NMR, δ (ppm): 7.07 (s, Ar-H of terminal PPO away from Ar-OH), 6.46 (s, Ar-H of internal PPO), 6.35 (s, Ar-H of terminal PPO next to Ar-OH), 4.28 (s, Ar-OH of terminal PPO), 2.15–2.02 (s, Ar-CH_3 of PPO).

EPPO (0.6), ^{1}H-NMR, δ (ppm): 7.07 (s, Ar- H of terminal PPO away from Ar-OH), 6.46 (s, Ar-H of internal PPO), 6.35 (s, Ar-H of terminal PPO next to Ar-OH), 4.28 (s, Ar-OH of terminal PPO), 3.99–3.95, 3.70–3.65, 3.31, 2.84, 2.67 (m, glycidyl ether protons), 2.19–2.02 (s, Ar-CH_3 of PPO).

EPPO (1.0), ^{1}H-NMR, δ (ppm): 7.07 (s, Ar-H of terminal PPO away from Ar-OH), 6.46 (s, Ar-H of internal PPO), 6.35 (s, Ar-H of terminal PPO next to Ar-OH), 3.99–3.95, 3.70–3.65, 3.31, 2.84, 2.67 (m, glycidyl ether protons), 2.19–2.02 (s, Ar-CH_3 of PPO).

The spectrum of original PPO exhibits a resonance peak of terminal hydroxyl proton at ~ 4.3 ppm. When the temperature of epoxidation reaction is 70°C (run 1), the area for the terminal hydroxyl proton decreases and the resonance peaks of epoxy proton is present. By comparing the peak areas of hydroxyl and epoxy protons, the conversion of terminal group is calculated to be 64.7%. With increasing the reaction temperature to 90°C, the peak for the terminal hydroxyl group of PPO disappears, indicative of the quantitative conversion of chain terminals. NMR results demonstrate that the terminal of PPO is successfully functionalized by epoxide in the used synthesis procedure. The remarkable increase in the conversion of terminal reaction from run 1 to 2 is ascribed to the increased reaction temperature.

Applied Polymer SCIENCE

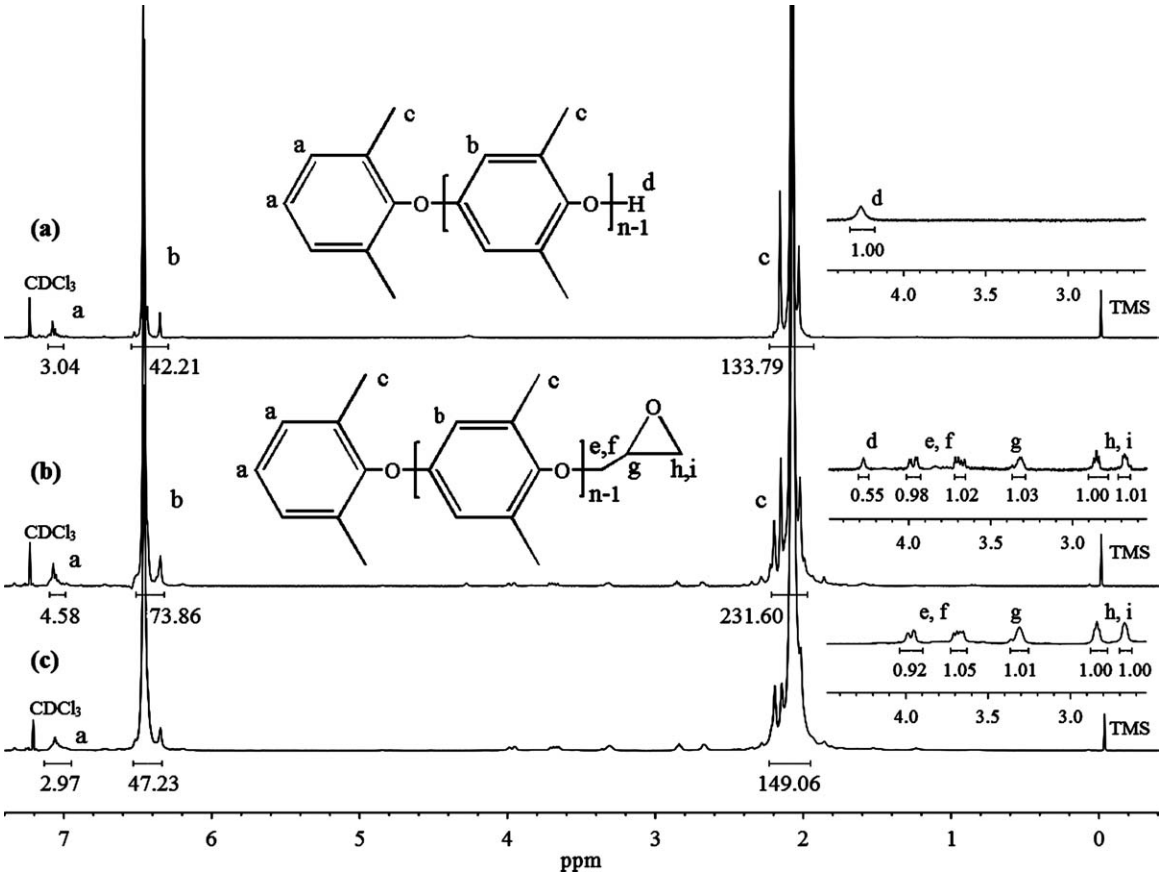

Figure 1. ^{1}H-NMR spectra of unmodified and terminally modified PPOs: (a) PPO, (b) EPPO (0.6), and (c) EPPO (1.0).

The M_n of PPO can be estimated by comparing the peak area of proton in terminal hydroxyl or epoxide groups with that of methyl, as shown in Table II. The M_n values evaluated from NMR are consistent with those measured via GPC. The molecular weight of PPO increases and its distribution narrows after the terminal modification, which might imply the successful transformation of chain terminals. The other reason for this may be due to the dissolution of EPPO with the extreme low molecular weight during precipitation into methanol.

Curing Behavior

The curing process of EPN/EPPO blends was investigated by FTIR analysis. Figure 2 shows the FTIR spectra of EPN/EPPO blends before and after curing. As seen in this figure, the characteristic bands of EPN at 916 cm^{-1} (the stretching vibration mode of epoxide) and curing agent DDS at 3460 and 3370 cm^{-1} (the asymmetric and symmetric stretching vibration modes of amine) disappear, and the intensity of the stretching vibration band of hydroxyl group around 3420 cm^{-1} increases after curing,[15,16] indicating the occurrence of curing reaction between epoxide and amine. The hydroxyl was generated through the addition reaction between epoxy and amine. With an increase of the EPPO content, the characteristic absorption of EPPO at 1184 cm^{-1} increases and that of EPN at 1600 and

Table II. Molecular Weights of PPO and EPPO

Sample	M_n (NMR)	M_n (GPC)	PDI (GPC)
PPO	2667	2694	2.26
EPPO (0.6)	2966	2973	2.07
EPPO (1.0)	2980	2999	2.04

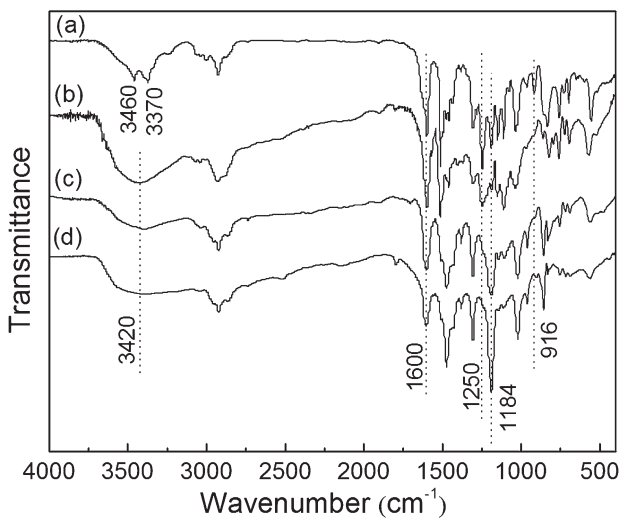

Figure 2. FTIR spectra of EPN/EPPO blends with different EPPO contents: (a) EPN/EPPO-0.1/DDS blend before curing, (b) EPN/EPPO-0.1, (c) EPN/EPPO-0.3, (d) EPN/EPPO-0.5 blends after curing.

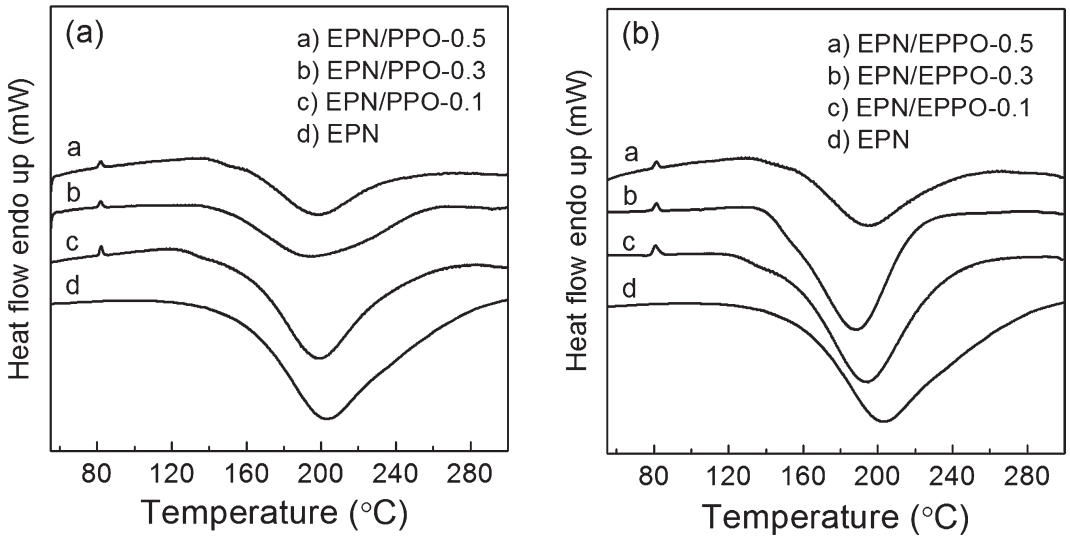

Figure 3. DSC curves recorded in the nonisothermal curing process of (a) EPN/PPO and (b) EPN/EPPO blends with different compositions.

1250 cm^{-1} decreases. The EPN/PPO blends show the similar variation tendency in FTIR spectra (data not shown).

The effects of terminal modification of PPO on the nonisothermal and isothermal curing kinetics of the blends were studied via DSC. Figure 3 shows the DSC curves of neat EPN, EPN/PPO, and EPN/EPPO blends recorded in the heating process. Each curve shows an exothermal curing peak in the temperature range of 120–280°C. The peak temperature (T_p) and ΔH_c were evaluated and plotted as a function of the blend composition in panels a and b of Figure 4, respectively. As seen in Figures 3 and 4(a), T_p decreases with the PPO or EPPO contents when the PPO or EPPO fraction is less than 0.3, which can be more clearly seen in the EPN/EPPO blends. This may suggest the catalytic effects of PPO on the curing of EPN. It has been reported that PPO acts as a catalyst for the curing of CE and the addition of PPO decreases the nonisothermal curing temperature of CE due to an autocatalytic curing mechanism.[28–30] However, T_p decreases with a further increase of PPO or EPPO fraction from 0.3 to 0.5, because of the steric hindrance effects of macromolecular blend component on the curing of EPN.[31,32]

As shown in Figure 4(b), the ΔH_c of EPN, which is proportional to the degree of curing, decreases with an increase in the fraction of PPO or EPPO, because the PPO or EPPO hinders the reaction and diffusion of EPN macromolecules during curing. Under the same blend compositions, the EPN/EPPO blends have lower T_p and higher ΔH_c values than the corresponding EPN/PPO blends, indicative of the faster curing rate and higher degree of curing of the former.

The isothermal curing behavior of EPN/PPO and EPN/EPPO blends was also studied via DSC. Figure 5 shows the DSC curves of neat EPN and its blends with different compositions recorded in the isothermal process at 180°C. As seen in this figure, a rapid increase in the reaction rate in the initial stage can

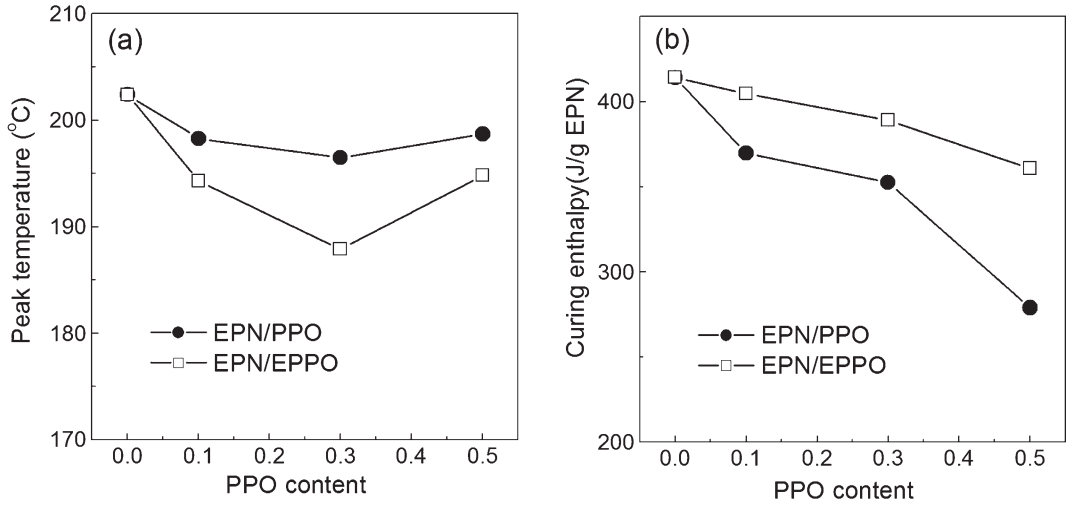

Figure 4. (a) Peak temperature and (b) curing enthalpy in the nonisothermal curing processes of EPN/PPO and EPN/EPPO blends with different compositions.

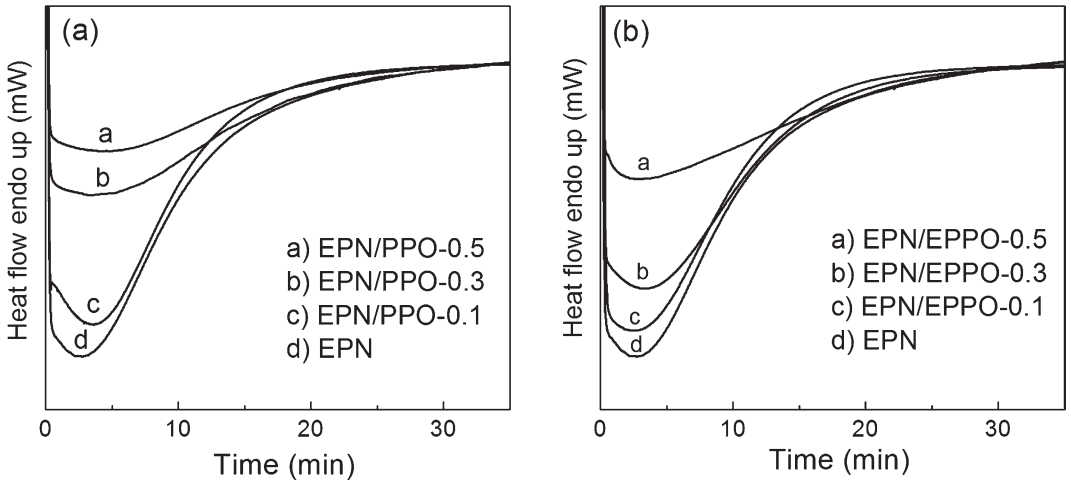

Figure 5. DSC curves recorded in the isothermal curing process of (a) EPN/PPO and (b) EPN/EPPO blends with different compositions at 180°C.

be observed, attributable to the auto-acceleration process arising from the hydroxyl groups formed during curing.[32,33] The isothermal heat flow curve was integrated to determine the relative conversion of curing (α) as a function of curing time (t). The α value at a given time t is calculated from

$$\alpha = \Delta H_t / \Delta H_{\text{total}}$$

where ΔH_t is the integrated area of the DSC curve from $t = 0$ to $t = t$ and ΔH_{total} is the integrated area of the whole heat flow curve. Figure 6 shows the plots of $\alpha \sim t$ for neat EPN, EPN/PPO, and EPN/EPPO blends with different compositions. Each curve of $\alpha \sim t$ plot shows a rapid increase of α in the early stage of curing, due to the auto-acceleration curing mechanism.[32,33] The $\alpha \sim t$ curve levels off to a plateau in the latter stage of curing, implying a cessation of curing as the system vitrifies.

On the basis of the $\alpha \sim t$ curves, the half curing time ($t_{1/2}$) was calculated, which corresponded to the time with 50% of conversion of curing. Figure 7 shows the $t_{1/2}$ and isothermal curing enthalpy of EPN/PPO and EPN/EPPO blends with different compositions. As seen in Figure 7(a), the $t_{1/2}$ value first decreases and then increases with an increase of the PPO or EPPO fraction, meaning the increase and decrease of curing rate at low and high PPO or EPPO content, respectively. It is considered that the PPO and EPPO played a dual role of catalysis and steric hindrance during curing of the blends. Besides, the isothermal curing enthalpy decreases with increasing PPO or EPPO content, due to the steric hindrance of PPO or EPPO chains on the curing of EPN. The variation tendencies of $t_{1/2}$ and ΔH_c in the isothermal curing process agree with the aforementioned nonisothermal DSC results.

At the same blend composition, the EPN/EPPO blends have smaller $t_{1/2}$ and larger ΔH_c than the EPN/PPO ones, indicating the faster and higher degree of curing of the reactive EPN/EPPO blends. Both the nonisothermal and isothermal DSC results suggest that the terminal epoxide groups of EPPO take part in the curing reaction and the terminally modified PPO

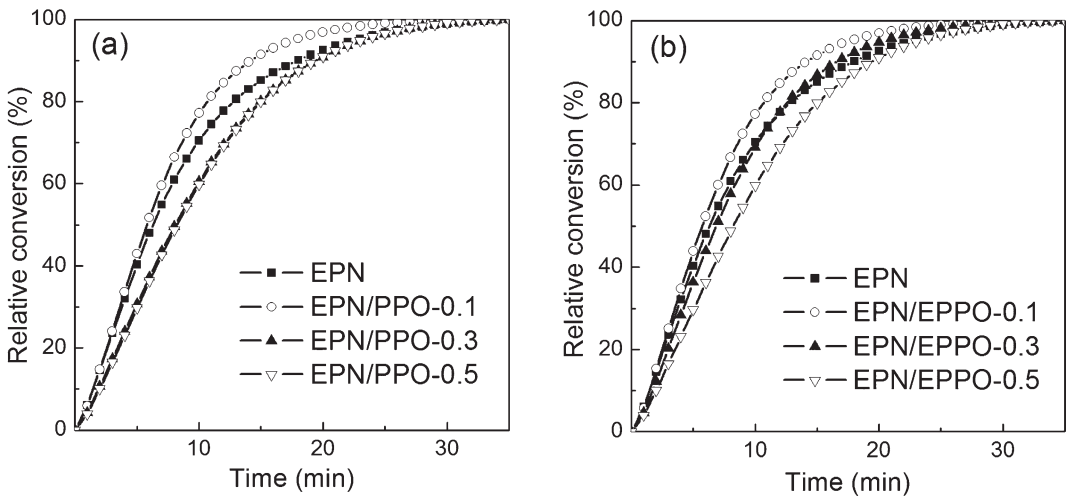

Figure 6. The α–t curves for isothermal curing of (a) EPN/PPO and (b) EPN/EPPO blends with different compositions.

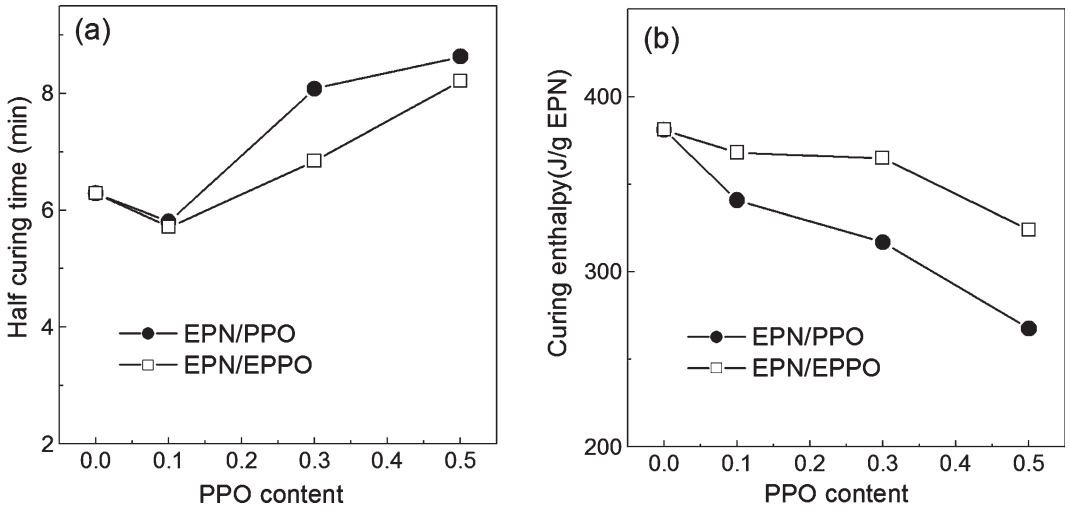

Figure 7. (a) Half curing time and (b) curing enthalpy in the isothermal curing processes of EPN/PPO and EPN/EPPO blends with different compositions.

has a smaller steric hindrance effects on the curing process than the unmodified one. Therefore, it is considered that the reactive blending of epoxide-functionalized PPO and epoxy resin is an efficient approach to promote the curing rate and degree of curing.

Phase Morphology

The effects of terminal modification of PPO on phase morphology of the blends were investigated via SEM. Figure 8 shows the SEM micrographs of cryofracture surfaces of nonetched (top) and etched with chloroform (bottom) for EPN/PPO blends. Figure 9 shows the corresponding SEM micrographs of the EPN/EPPO blends. As shown in Figure 8, the phase morphology cannot be clearly seen in the nonetched specimen. The morphological features of the blends can be seen after etching with chloroform. At a low PPO content (e.g., 10%), EPN is the continuous phase, in which the PPO component is dispersed as the irregular-shaped islands. As the PPO content increases, the

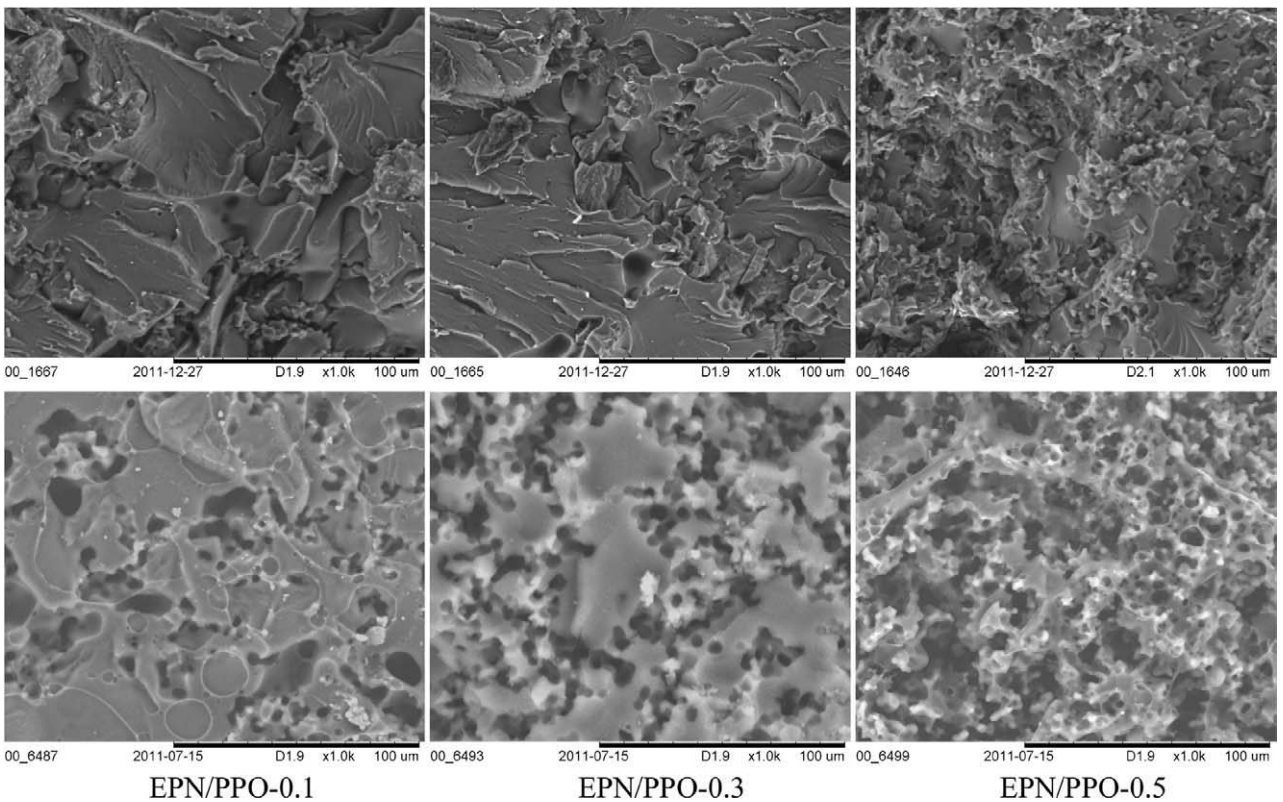

Figure 8. SEM micrographs of nonetched (top) and etched (bottom) EPN/PPO blends with different compositions.

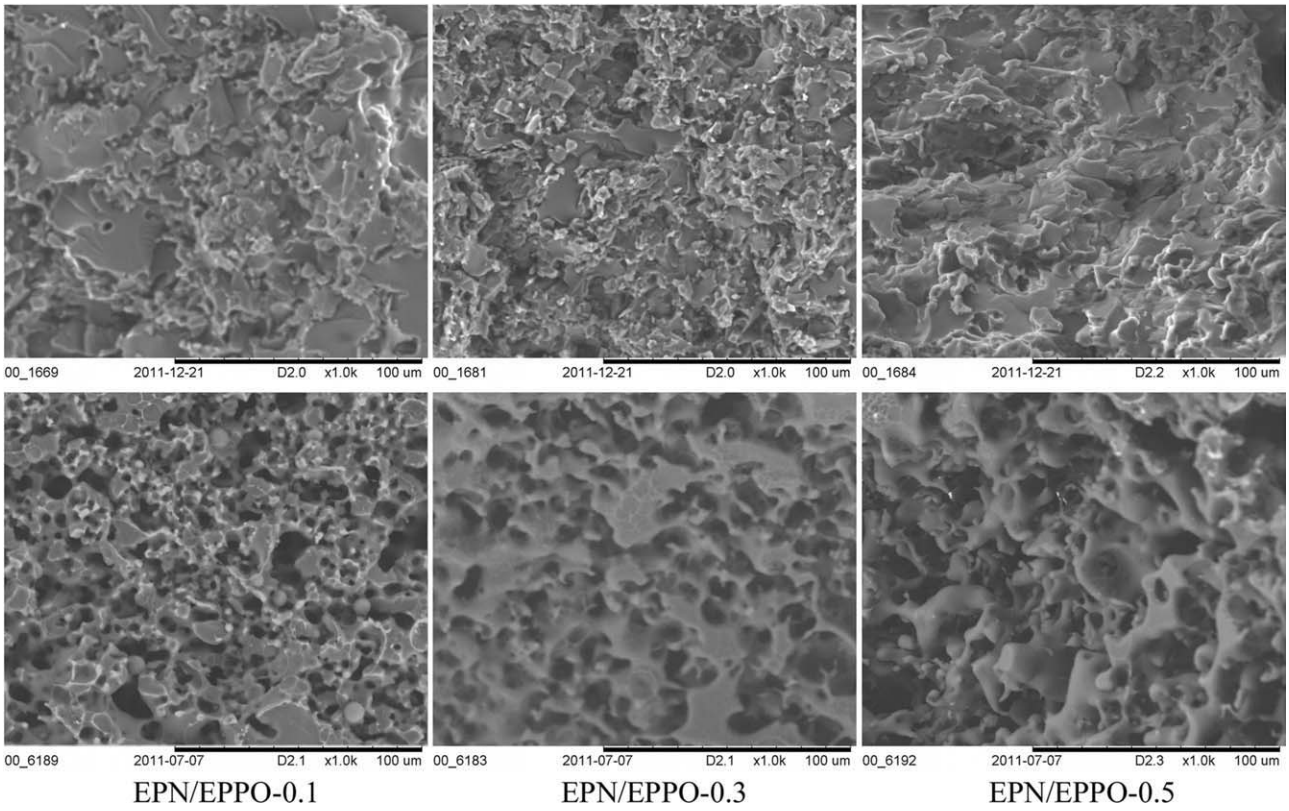

Figure 9. SEM micrographs of nonetched (top) and etched (bottom) EPN/EPPO blends with different compositions.

size of dispersed phase becomes smaller and more regular, and tends to overlap and coalesce. When the PPO content is increased to 50%, the PPO phase changes to the ribbon-like shapes and a co-continuous morphology is generated. The morphology development of the blends can be explained by the mass transfer mechanism.[7] The transfer of PPO phase is restrained by the cross-linked structure of EPN. Accordingly, the PPO phase is dispersed as the islands in the EPN matrix at a low content, while the sites of phase-separated PPO tend to overlap, coalesce, and form a co-continuous phase at a high PPO content.

For the EPN/PPO blends, the low-molecular-weight PPO can improve the miscibility of blends due to the entropic contribution.[10] On the other hand, as predicted by the Flory–Huggins theory, the curing reaction can induce the phase separation because of the formation of cross-linked structure and the increase of EPN molecular weight, which leads to the decrease of entropy.[11] Due to the reaction between the blend pair in curing, the EPN/EPPO blends give rise to the interesting morphological features after curing. As shown in Figure 9, after etching the fracture surface, EPPO phase is dispersed throughout the EPN matrix and a nearly co-continuous morphology is generated even at a very low EPPO concentration (10%). The fuzzier phase interface and more obvious co-continuous morphology are observed with an increase in the EPPO content. The unique morphology of EPN/EPPO blends can be ascribed to the reaction between the terminal epoxide of EPPO and diamine. For the reactive EPN/EPPO blends, EPPO can be involved in the cross-linked structure of EPN matrix and a co-continuous phase is ultimately generated at a relatively low EPPO content. On the other hand, SEM results indicate that only part of EPPO reacts with DDS in the curing process. The curing system has extremely high viscosity, which may impact the diffusion of blend component and curing agent. Therefore, EPPO cannot react with DDS completely, although the DDS is slightly excessive compared to the epoxy groups of EPN and EPPO.

Physical Properties

The thermal stability, dielectric property, and water adsorption behavior of the EPN/EPPO blends were also investigated. Figure 10 shows the TGA curves of neat EPN and its reactive blends with EPPO. $T_{d,5\%,}$ which corresponds to the temperature with 5 wt% weight loss and is close to the onset temperature of decomposition, is used to evaluate the thermal stability. Both EPN and EPPO have excellent thermal stability, because they bear the high-density benzene ring structure. The $T_{d,5\%}$ value of EPN is 392.3°C, a little lower than that of EPPO (412.5°C). The $T_{d,5\%}$ values of EPN/EPPO blends with 0.1, 0.3, and 0.5 EPPO fractions are 395.6°C, 406.9°C, and 396.7°C, respectively. It first increases and then decreases as the content of EPPO increases. The slight decrease in $T_{d,5\%}$ of EPN/EPPO blends at high EPPO content might be due to the decreased degree of curing under this condition. Interestingly, the residual weight percentage at 700°C is ca. 44% for neat EPN, while it decreases to 25–27% for the blends and is almost unvaried with a further increase of EPPO content, meaning that EPPO promotes the full decomposition of EPN at a high temperature.

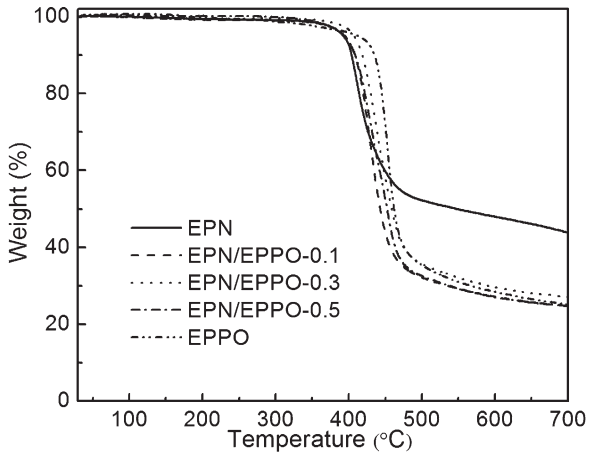

Figure 10. TGA curves of EPN/EPPO blends as a function of EPPO content.

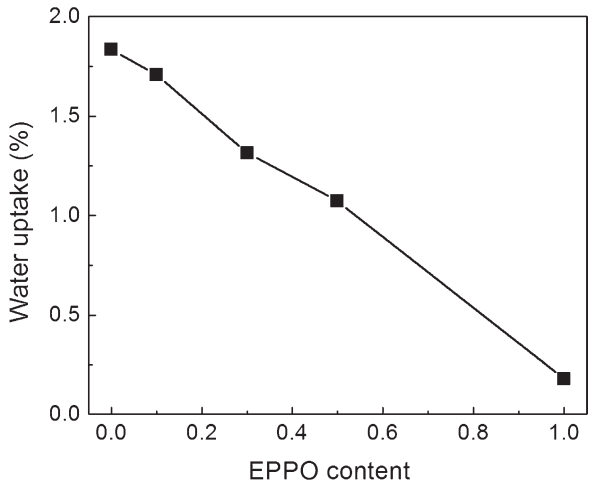

Figure 12. Water uptake of EPN/EPPO blends as a function of EPPO content.

The dielectric properties of EPN/EPPO blends were determined by the parallel-plate capacitor method. Figure 11 shows the dielectric constant (D_k) and dissipation factor (D_f) of the blends with different compositions. As seen in this figure, the blends have remarkable lower D_k and D_f than neat EPN, and the D_k and D_f values generally decreases with increasing the EPPO content. This is due to the fact that the bulky, low-polar, and symmetric phenylene oxide groups in the EPPO polymer chains shield the interchain electronic interactions and increase the hydrophobicity.[15] However, the D_k and D_f values remain nearly constant when the EPPO fraction is increased from 0.3 to 0.5, which is considered to be attributed to the multiphase morphology of the blends.[28] In the case of a multiphase material, the dielectric properties are mainly dominated by the polarity of each phase and those interfaces in subsurface (the area immediately next to the sample surfaces) of the material. The appearance of the second phase increases the quantity of the accumulated charge due to an additional contribution from the polarization of phase interfaces.[28] These results suggest that the dielectric properties of EPN/EPPO blends are not only composition but also morphology dependent.

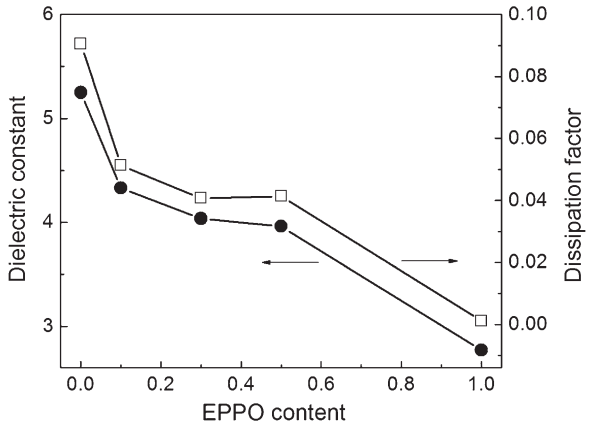

Figure 11. Dielectric property of EPN/EPPO blends as a function of EPPO content.

Generally, the water uptake has a negative effect on the physical performances of polymer resin such as the thermal stability and dielectric property. Since water possesses a much higher D_k value (ca. 78) than the polymeric matrix, the absorption of a small amount of water in resins can dramatically impact their dielectric properties. Figure 12 shows the water absorption of EPN/EPPO blends after immersion into the boiling water for 48 h. The water uptake of EPN/EPPO blends is significantly lower than that of neat EPN and it decreases with increasing the EPPO fraction. The low-water uptake is attributed to the presence of low polar and symmetric phenylene oxide groups in the polymer chain of EPPO.[15,16]

CONCLUSIONS

In this study, the chain ends of PPO were successfully modified to epoxide. The conversion of epoxidation reaction of the PPO terminal groups can be controlled by the reaction temperature and the quantitative conversion is attained at a relatively high temperature (90°C). FTIR and DSC results indicate that the terminally epoxide-modified PPO takes part in the curing reaction of EPN. As revealed in the nonisothermal and isothermal curing kinetic studies, the curing rates of EPN/PPO and EPN/EPPO blends first increase and then decrease with increasing the PPO or EPPO fraction. Due to the steric hindrance effects of PPO and EPPO, the blends have lower degree of curing than neat EPN. The EPN/EPPO reactive blends have faster curing rate and higher degree of curing than the corresponding EPN/PPO blends. Compared to the typical sea-island morphology of the EPN/PPO blends, a co-continuous phase is generated in the EPN/EPPO blends even at a low EPPO content. The EPN/EPPO blends have excellent thermal stability due to the high density of the benzene ring structure. The dielectric constant, dissipation factor, and water uptake of EPN/EPPO blends are remarkably lower than those of neat EPN. The results shown in this study suggest that the EPN/EPPO reactive blend could be a promising material for the high-performance electronic products.

ACKNOWLEDGMENTS

The authors acknowledge the financial supports of the Natural Science Foundation of China (20974100 and 20674075) and Natural Science Foundation of Zhejiang Province (Y404299).

REFERENCES

1. Lin, C.-H.; Wang, C.-S. *Polymer* **2001,** *42*, 1869.
2. Sharmin, E.; Alam, M. S.; Philip, R. K.; Ahmad, S. *Prog. Org. Coat.* **2010,** *67*, 170.
3. Maier, G. *Prog. Polym. Sci.* **2001,** *26*, 3.
4. Huang, C.-C.; Yang, M.-S.; Liang, M. *J. Polym. Sci. Part A: Polym. Chem.* **2006,** *44*, 5875.
5. Su, C.-T.; Lin, K.-Y.; Lee, T.-J.; Liang, M. *Eur. Polym. J.* **2010,** *46*, 1488.
6. Liang, G.; Meng, J.; Zhao, L. *Polym. Int.* **2003,** *52*, 966.
7. Merfeld, G. D.; Yeager, G. W.; Chao, H. S.; Singh, N. *Polymer* **2003,** *44*, 4981.
8. Venderbosch, R. W.; Meijer, H. E. H.; Lemstra, P. *J. Polymer* **1994,** *35*, 4349.
9. Prolongo, S. G.; Cabanelas, J. C.; Fine, T.; Pascault, J. *J. Appl. Polym. Sci.* **2004,** *93*, 2678.
10. Soulé, E. R.; Fine, T.; Borrajo, J.; Williams, R. J. J.; Pascault, J. P. *J. Appl. Polym. Sci.* **2006,** *100*, 1742.
11. Ishii, Y.; Ryan, A. J.; Clarke, N. *Polymer* **2003,** *44*, 3641.
12. Wu, S.-J.; Lin, T.-K.; Shyu, S.-S. *J. Appl. Polym. Sci.* **2000,** *75*, 26.
13. Wu, S.-J.; Tung, N.-P.; Lin, T.-K.; Shyu, S.-S. *Polym. Int.* **2000,** *49*, 1452.
14. Chao, H. S.-I.; Whalen, J. M. *J. Appl. Polym. Sci.* **1993,** *49*, 1537.
15. Hwang, H.-J.; Hsu, S.-W.; Wang, C.-S. *J. Appl. Polym. Sci.* **2008,** *110*, 1880.
16. Hwang, H.-J.; Hsu, S.-W.; Chung, C.-L.; Wang, C.-S. *React. Funct. Polym.* **2008,** *68*, 1185.
17. Wang, C.-S.; Lee, M.-C. *J. Appl. Polym. Sci.* **1999,** *73*, 1611.
18. Ho, T.-H.; Hwang, H.-J.; Shieh, J.-Y.; Chung, M.-C. *React. Funct. Polym.* **2009,** *69*, 176.
19. Wu, S.-J. *J. Appl. Polym. Sci.* **2006,** *102*, 1139.
20. Chen, F. H.; Wang, X.; Zhao, X. J.; Liu, J. G.; Yang, S. Y.; Han, C. C. *Macromol. Rapid Commun.* **2008,** *29*, 74.
21. Jin, F.-L.; Park, S.-J. *J. Polym. Sci. Part B: Polym. Phys.* **2006,** *44*, 3348.
22. Monticelli, O.; Fina, A.; Ullah, A.; Waghmare, P. *Macromolecules* **2009,** *42*, 6614.
23. Jiang, G. J.; Wu, H.; Guo, S. Y. *Polym. Eng. Sci.* **2010,** *50*, 2273.
24. Yi, F. P.; Yu, R. T.; Zheng, S. X.; Li, X. H. *Polymer* **2011,** *52*, 5669.
25. Liu, Y. L.; Wu, C. S.; Hsu, K. Y.; Chang, T. H. *J. Polym. Sci. Part A: Polym. Chem.* **2002,** *40*, 2329.
26. Mathew, D.; Nair, C. P. N.; Ninan, K. N. *J. Appl. Polym. Sci.* **1999,** *74*, 1675.
27. Lee T.-J.; Fang Y.-D.; Yuan W.-G.; Wei, K.-M.; Liang, M. *Polymer* **2007,** *48*, 734.
28. Gao, R.; Gu, A. J.; Liang, G. Z.; Dai, S. K.; Yuan, L. *J. Appl. Polym. Sci.* **2011,** *121*, 1675.
29. Huang, P. Z.; Gu, A. J.; Liang, G. Z.; Yuan, L. *J. Appl. Polym. Sci.* **2011,** *121*, 2113.
30. Wu, S.-J.; Mi, F.-L. *Polym. Int.* **2006,** *55*, 1296.
31. Yao, D.; Kuila, T.; Sun, K.-B.; Kim, N.-H.; Lee, J.-H. *J. Appl. Polym. Sci.* **2012,** *124*, 2325.
32. Pillai, J. P.; Pionteck, J.; Haßler, R.; Sinturel, C.; Mathew, V. S.; Thomas, S. *Ind. Eng. Chem. Res.* **2012,** *51*, 2586.
33. Su, C. C.; Kuo, J.-F.; Woo, E. M. *J. Polym. Sci. Part B: Polym. Phys.* **1995,** *33*, 2235.